JOURNAL OF MULTIFUNCTIONAL MATERIALS & PHOTOSCIENCE
5(1), June 2014, pp. 21-29

Preparation and Upconversion Photoluminescence of $CaLa_2(MoO_4)_4$: Er^{3+}/Yb^{3+} Particles via Microwave-Modified Sol-Gel Route

Chang Sung Lim

Department of Advanced Materials Science & Engineering, Hanseo University
Seosan 356-706, Republic of Korea

Abstract: $CaLa_2(MoO_4)_4:Er^{3+}/Yb^{3+}$ phosphors were successfully prepared via microwave-modified sol-gel route, and the upconversion photoluminescence properties have been investigated. Well-crystallized particles, formed after heat-treatment at 900°C for 12 h, showed a fine and homogeneous morphology with particle sizes of 1-3 ìm. Under excitation at 980 nm, $CaLa_2(MoO_4)_4:Er^{3+}/Yb^{3+}$ phosphors exhibited a strong 525-nm emission band, a weak 550-nm emission band in the green region and a very weak 655-nm emission band in the red region. The Raman spectra of the particles indicated the presence of strong peaks at higher frequencies (1026, 1092 and 1316 cm^{-1}) and weak peaks at lower frequencies (236, 288, 365, 420 and 560 cm^{-1}) induced by the disorder of the $[MoO_4]^{2-}$ groups with the incorporation of the Er^{3+} and Yb^{3+} elements into the crystal lattice or by a new phase formation.

Keywords: $CaLa_2(MoO_4)_4:Er^{3+}/Yb^{3+}$, Microwave, Sol-Gel, Upconversion photoluminescence.

Introduction

Rare-earth-doped upconversion (UC) photoluminescence particles have attracted great attention because of the conversion from near infrared radiation of low energy to visible radiation of high energy. The UC photoluminescence particles have shown potential applications in various fields including biomedical imaging owing to their unique UC optical behaviors that offer improved light penetration depth, high chemical and photo stability, as well as the absence of auto-fluorescence during imaging, sharp emission bands, and high resistance to photobleaching, which overcome the current limitations in traditional photoluminescence materials [1-3].

The double molybdate compounds of $MR_2(MoO_4)_4$ (M: bivalent alkaline earth metal ion, R: trivalent rare earth ion) belong to a group of double alkaline earth lanthanide molybdates. With the decrease in the ionic radius of alkaline earth metal ions ($R_{ca} < R_{Sr} < R_{ba}$; R = ionic radius), the structure of $MR_2(MoO_4)_4$ could be transformed to a highly

*Corresponding author: *cslim@hanseo.ac.kr*

disordered tetragonal scheelite structure from the monoclinic structure. It is possible that that the trivalent rare earth ions in the disordered tetragonal-phase could be partially substituted by Er^{3+} and Yb^{3+} ions, and the ions are effectively doped into the crystal lattices of the tetragonal phase due to the similar radii of trivalent rare earth ions of R^{3+}, resulted in the excellent UC photoluminescence properties [4-6]. Among the rare earth ions, the Er^{3+} ion is suitable for converting infrared to visible light through the UC process due to proper electronic energy level configuration. The co-doped Yb^{3+} ion and Er^{3+} ion can remarkably enhance the UC efficiency from infrared to visible light due to the efficiency energy transfer from Yb^{3+} to Er^{3+}. The Yb^{3+} ion as a sensitizer can be effectively excited by incident light source energy that is transferred to the activator, from which radiation can be emitted. The Er^{3+} ion activator is the luminescence center of the UC particles, while the sensitizer enhances the UC luminescence efficiency [7-9].

Rare-earth activated $MR_2(MoO_4)_4$ (M = Ba, Sr, Ca; R = La, Gd, Y) have attracted great attention because of the their spectroscopic characteristics with excellent upconversion photoluminescence properties. Several processes have been developed to prepare the rare-earth-doped double molybdates, including solid-state reactions [9-14], co-precipitation [15, 16], sol-gel method [4-7], hydrothermal method [17, 18], Pechini method [19, 20], organic gel-thermal decomposition [21], and microwave-assisted hydrothermal method [22]. For practical application of UC photoluminescence in products such as lasers, three-dimensional displays, light-emitting devices, and biological detectors, features such as homogeneous UC particle size distribution and morphology need to be well defined. Usually, double molybdates were prepared by a solid-state method that requires high temperatures, lengthy heating process and subsequent grinding, which results in loss of the emission intensity and an increase in cost. Sol-gel process provides some advantages over the conventional solid-state method, including good homogeneity, low calcination temperature, small particle size and narrow particle size distribution optimal for good luminescent characteristics. However, the sol-gel process has a disadvantage in that it takes a long time for gelation. As compared with the usual methods, microwave synthesis has advantages of very short reaction time, small-size particles, narrow particle size distribution, and high purity of final polycrystalline samples. Microwave heating is delivered to the material surface by radiant and/or convection heating, which is transferred to the bulk of the material via conduction [23, 24]. A cyclic microwave-modified sol-gel process is a cost-effective method that provides high homogeneity with easy scale-up, and it is emerging as a viable alternative approach for the synthesis of high-quality luminescent materials in short time periods.

In this study, Er^{3+} doped $CaLa_2(MoO_4)_4$ and Er^{3+}/Yb^{3+} co-doped $CaLa_2(MoO_4)_4$ phosphors were prepared via cyclic microwave- modified sol-gel route followed by heat treatment. The synthesized particles were characterized by X-ray diffraction (XRD), scanning electron microscopy (SEM), and energy-dispersive X-ray spectroscopy (EDS). The optical properties were examined comparatively using photoluminescence (PL) emission and Raman spectroscopy.

Experimental

Appropriate stoichiometric amounts of $Ca(NO_3)_2 \cdot 4H_2O$ (99%, Sigma-Aldrich, USA), $La(NO_3)_3 \cdot 6H_2O$ (99%, Sigma-Aldrich, USA), $(NH_4)_6Mo_7O_{24} \cdot 4H_2O$ (99%, Alfa Aesar, USA), $Er(NO_3)_3 \cdot 5H_2O$ (99.9%, Sigma-Aldrich, USA), $Yb(NO_3)_3 \cdot 5H_2O$ (99.9%, Sigma-Aldrich, USA), citric acid (99.5%, Daejung Chemicals, Korea), NH_4OH (A.R.), ethylene glycol (A.R.) and distilled water were used to prepare $CaLa_2(MoO_4)_4$, $CaLa_2(MoO_4)_4$: Er^{3+}, $CaLa_2(MoO_4)_4$:Er^{3+}/Yb^{3+} and $CaLa_2(MoO_4)_4$: Er^{3+},Yb^{3+}# compounds with the doping concentrations of Er^{3+} and Yb^{3+} (Er^{3+} = 0.05, 0.1, 0.2 and Yb^{3+} = 0.2, 0.45). To prepare $CaLa_2(MoO_4)_4$, 0.4 mol% $Ca(NO_3)_2 \cdot 4H_2O$ and 0.4 mol% $(NH_4)_6Mo_7O_{24} \cdot 4H_2O$ were dissolved in 20 mL of ethylene glycol and 80 mL of 5M NH_4OH under vigorous stirring and heating. Subsequently, 0.8 mol% $La(NO_3)_3 \cdot 6H_2O$ and citric acid (with a molar ratio of citric acid to total metal ions of 2:1) were dissolved in 100 mL of distilled water under vigorous stirring and heating. Then, the solutions were mixed together under vigorous stirring and heating. At the end, the highly transparent solutions were obtained and adjusted to pH=7-8 by the addition of 8M NH_4OH. In the second way, to prepare $CaLa_2(MoO_4)_4$: Er^{3+}, the mixture of 0.72 mol% $La(NO_3)_3 \cdot 6H_2O$ with 0.08 mol% $Er(NO_3)_3 \cdot 5H_2O$ was used for creation of the rare earth solution. In the third way, to prepare $CaLa_2(MoO_4)_4$:Er^{3+},Yb^{3+}, the mixture of 0.68 mol% $La(NO_3)_3 \cdot 6H_2O$ with 0.04 mol% $Er(NO_3)_3 \cdot 5H_2O$ and 0.08 mol% $Yb(NO_3)_3 \cdot 5H_2O$ was used for creation of the rare earth solution. In the fourth way, to prepare $CaLa_2(MoO_4)_4$: Er^{3+},Yb^{3+}#, the rare earth containing solution was generated using 0.6 mol% $La(NO_3)_3 \cdot 6H_2O$ with 0.02 mol% $Er(NO_3)_3 \cdot 5H_2O$ and 0.18 mol% $Yb(NO_3)_3 \cdot 5H_2O$.

The transparent solutions were placed into a microwave oven operating at a frequency of 2.45 GHz with a maximum output-power of 1250 W for 30 min. The working cycle of the microwave reaction was controlled very precisely between 40 s on and 20 s off for 15 min, followed by further treatment of 30 s on and 30 s off for 15 min. The ethylene glycol was evaporated slowly at its boiling point. Ethylene glycol is a polar solvent at its boiling point of 197°C, and this solvent is a good candidate for the microwave process. Respectively, if ethylene glycol is used as the solvent, the reactions proceed at the boiling point temperature. When microwave radiation is supplied to the ethylene-glycol-based solution, the components dissolved in the ethylene glycol can couple. The charged particles vibrate in the electric field interdependently, when a large amount of microwave radiation is supplied to the ethylene glycol. The samples were treated with ultrasonic radiation for 10 min to produce a light yellow transparent sol. After this stage, the light yellow transparent sols were dried at 120°C in a dry oven for 48 h to obtain black dried gels. The black dried gels were grinded and heat-treated at 900°C for 12 h with 100°C interval between 600-900°C. Finally, the white particles were obtained for $CaLa_2(MoO_4)_4$ with pink particles for $CaLa_2(MoO_4)_4$:Er^{3+}, $CaLa_2(MoO_4)_4$:Er^{3+}/Yb^{3+} and $CaLa_2(MoO_4)_4$:Er^{3+}/Yb^{3+}# compositions.

The phase composition of the synthesized particles was identified using XRD (D/MAX 2200, Rigaku, Japan). The microstructure and surface morphology of the synthesized particles were observed using SEM/EDS (JSM-5600, JEOL, Japan). The PL spectra were recorded using a spectrophotometer (Perkin Elmer LS55, UK) at room temperature. Raman

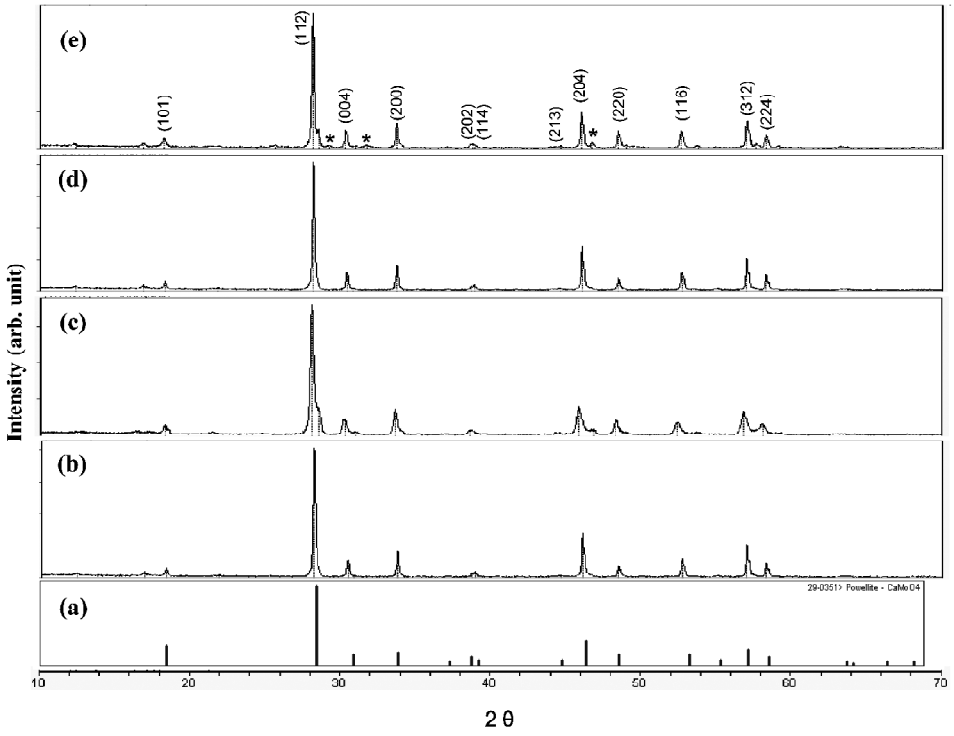

Figure 1: X-ray diffraction patterns of the (a) JCPDS 29-0351 data of $CaMoO_4$, the synthesized (b) $CaLa_2(MoO_4)_4$, (c) $CaLa_2(MoO_4)_4:Er^{3+}$, (d) $CaLa_2(MoO_4)_4:Er^{3+}/Yb^3$ and (e) $CaLa_2(MoO_4)_4:Er^{3+}/Yb^{3+}$# particles.

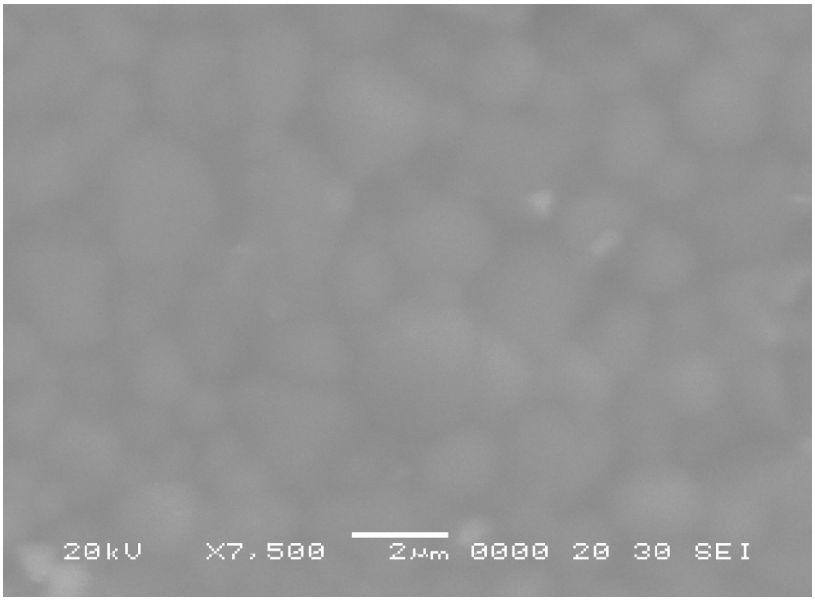

Figure 2: Scanning electron microscopy images of the synthesized $CaLa_2(MoO_4)_4:Er^{3+}/Yb^{3+}$# particles.

(a)

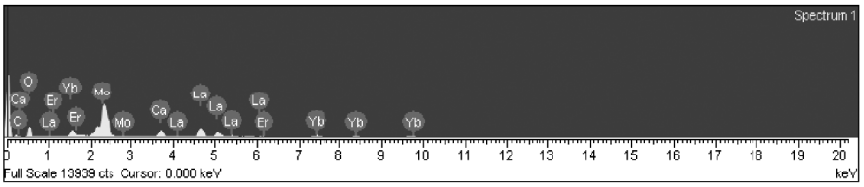

(b)

Spectrum	In stats.	C	O	Ca	Mo	La	Er	Yb	Total
Spectrum 1	Yes	16.37	32.20	2.69	28.00	13.63	0.80	6.32	100.00
Spectrum 2	Yes	15.29	32.39	2.64	28.77	13.99	0.67	6.25	100.00
Spectrum 3	Yes	17.49	32.43	2.53	27.01	13.30	0.68	6.57	100.00
Spectrum 4	Yes	15.88	33.08	2.62	27.96	13.33	0.59	6.54	100.00
Mean		16.25	32.53	2.62	27.94	13.56	0.68	6.42	100.00
Std. deviation		0.93	0.38	0.07	0.72	0.32	0.08	0.16	
Max.		17.49	33.08	2.69	28.77	13.99	0.80	6.57	
Min.		15.29	32.20	2.53	27.01	13.30	0.59	6.25	

(c)

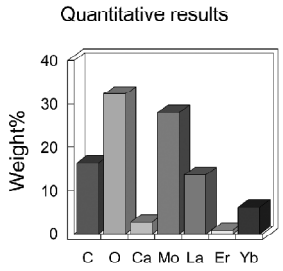

Figure 3: Energy-dispersive X-ray spectroscopy patterns (a), quantitative compositions (b) and quantitative results (c) of the synthesized $CaLa_2(MoO_4)_4$: Er^{3+}/Yb^{3+}# particles.

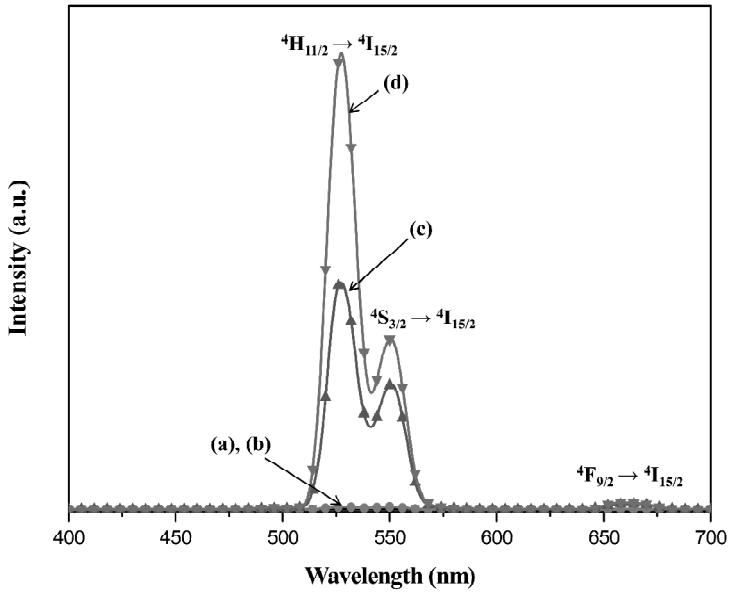

Figure 4: Upconversion photoluminescence emission spectra of (a) $CaLa_2(MoO_4)_4$, (b) $CaLa_2(MoO_4)_4$:Er^{3+}, (c) $CaLa_2(MoO_4)_4$:Er^{3+}/Yb^{3+} and (d) $CaLa_2(MoO_4)_4$:Er^{3+}/Yb^{3+}# particles excited under 980 nm at room temperature.

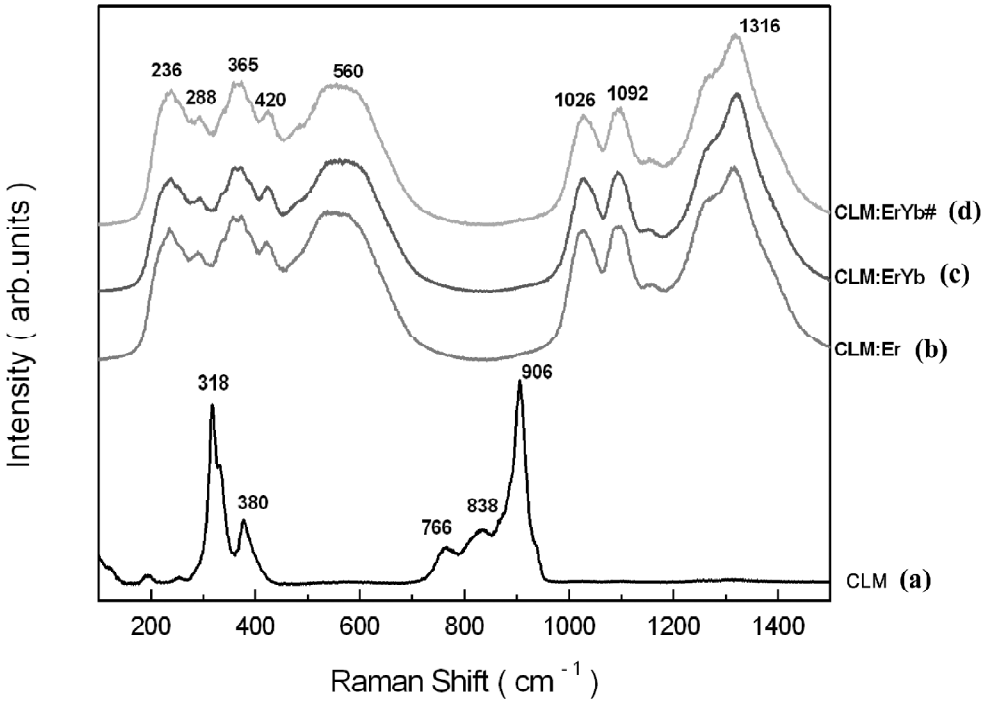

Figure 5: Raman spectra of the synthesized (a) $CaLa_2(MoO_4)_4$(CLM), (b) $CaLa_2(MoO_4)_4$:Er^{3+}(CLM:Er), (c) $CaLa_2(MoO_4)_4$:Er^{3+}/Yb^{3+}(CLM:ErYb) and (d) $CaLa_2(MoO_4)_4$:Er^{3+}/Yb^{3+}#(CLM:ErYb#) particles excited by the 514.5-nm line of an Ar ion laser at 0.5 mW on the samples.

spectroscopy measurements were performed using a LabRam Aramis (Horiba Jobin-Yvon, France). The 514.5-nm line of an Ar ion laser was used as an excitation source, and the power on the samples was kept at 0.5 mW.

Results and Discussion

Fig. 1 shows the XRD patterns of the (a) JCPDS 29-0351 data of $CaMoO_4$, the synthesized (b) $CaLa_2(MoO_4)_4$, (c) $CaLa_2(MoO_4)_4$: Er^{3+}, (d) $CaLa_2(MoO_4)_4$: Er^{3+}/Yb^3 and (e) $CaLa_2(MoO_4)_4$: Er^{3+}/Yb^{3+}# particles. The crystal structure of $CaLa_2(MoO_4)_4$ has not been existed in JCPDS data. However, the XRD peaks in Fig 1 are similar with the phase based on the tetragonal $CaMoO_4$ with a scheelite-type structure of space group $I4_1/a$ with lattice parameters of a = b = 5.212 Å and c = 11.438 Å [25-26], which was in good agreement with the crystallographic data of $CaMoO_4$ (JCPDS 29-0351). Impurity phases were detected at 25°, 29.5°, 31.5° and 46.5° in Fig. 1(e). The foreign reflexes are marked with asterisk in Fig. 1(e) when the doping concentration of Er^{3+}/Yb^{3+} is 0.02/0.18 mol%. The similar impurity phase was also observed in the case of Er^{3+}/Yb^{3+} doped $CaMoO_4$ phosphor when the doping concentration of Er^{3+}/Yb^{3+} is 0.02/0.18 mol% [26]. The foreign reflexes marked with asterisk in Fig. 1(e) compared to the (a) JCPDS 29-0351 data of $CaMoO_4$ can be ascribed that La^{3+}, Er^{3+} and Yb^{3+} ions are well substituted in the tetragonal-phase $CaMoO_4$ of the scheelite-type structure, and form a new phase induced by the disorder of the $[MoO_4]^{2-}$ groups.

This suggests that the cyclic microwave-modified sol-gel route is suitable for the growth of $CaLa_2(MoO_4)_4$:Er^{3+}/Yb^{3+} crystallites and for developing the strongest intensity peaks at the (112), (204), and (312) planes, which are the major peaks of $CaMoO_4$ [25, 26]. Post heat-treatment plays an important role in a well-defined crystallized morphology. To achieve a well-defined crystalline morphology, the $CaLa_2(MoO_4)_4$, $CaLa_2(MoO_4)_4$:Er^{3+}, $CaLa_2(MoO_4)_4$:Er^{3+}/Yb^3 and $CaLa_2(MoO_4)_4$:Er^{3+}/Yb^{3+}# phases need to be heat treated at 900°C for 12 h. It is assumed that the doping amount of Er^{3+}/Yb^{3+} has a great effect on the crystalline cell volume of the $CaLa_2(MoO_4)_4$, because of the different ionic sizes and energy band gaps. This means that the obtained samples possess a tetragonal-phase after partial substitution of La^{3+} by Er^{3+} and Yb^{3+} ions, and the ions are effectively doped into crystal lattices of the $CaLa_2(MoO_4)_4$ phase due to the similar radii of La^{3+} and by Er^{3+} and Yb^{3+}.

Fig. 2 shows SEM images of the synthesized $CaLa_2(MoO_4)_4$: Er^{3+}/Yb^{3+}# particles. The as-synthesized samples are well crystallized with a fine and homogeneous morphology and particle size of 1-3 μm. The sample of $CaLa_2(MoO_4)_4$: Er^{3+},Yb^{3+}# have some inhomogeneous particles. It is noted that the doping amounts of Er^{3+} and Yb^{3+} has a great effect on the morphological features. Fig. 3 shows the (a) energy-dispersive X-ray spectroscopy patterns, (b) quantitative compositions and (c) quantitative results of the synthesized $CaLa_2(MoO_4)_4$: Er^{3+}/Yb^{3+}# particles. The EDS pattern (a) shows that the $CaLa_2(MoO_4)_4$: Er^{3+}/Yb^{3+}# particles are composed of Ca, La, Mo, O, Er and Yb. The quantitative compositions (b) show precise constitutions of the synthesized $CaLa_2(MoO_4)_4$: Er^{3+}/Yb^{3+}# particles. The quantitative results (c) are in good relation with nominal composition of the $CaLa_2(MoO_4)_4$: Er^{3+}/Yb^{3+}# particles. The relation of Ca, La, Mo, O, Er and Yb shows that the $CaLa_2(MoO_4)_4$: Er^{3+}/Yb^{3+}# particles can be successfully synthesized using the cyclic microwave-modified sol-gel method. The cyclic microwave-modified sol-gel process of double molybdates provides the energy to synthesize the bulk of the material uniformly, so that fine particles with controlled morphology can be fabricated in short time periods. The method is a cost-effective way to provide highly homogeneous products with easy scale-up, and it is a viable alternative for the rapid synthesis of UC particles.

Fig. 4 shows the UC photoluminescence emission spectra of the as-prepared (a) $CaLa_2(MoO_4)_4$, (b) $CaLa_2(MoO_4)_4$: Er^{3+}, (c) $CaLa_2(MoO_4)_4$: Er^{3+},Yb^{3+}, and (d) $CaLa_2(MoO_4)_4$: Er^{3+},Yb^{3+}# particles excited under 980 nm at room temperature. The strong 525-nm emission band and the weak 550-nm emission band in the green region correspond to the $^2H_{11/2} \rightarrow {}^4I_{15/2}$ and $^4S_{3/2} \rightarrow {}^4I_{15/2}$ transitions, respectively, while the very weak emission 655-nm band in the red region corresponds to the $^4F_{9/2} \rightarrow {}^4I_{15/2}$ transition. The UC intensities of (a) $CaLa_2(MoO_4)_4$ and (b) $CaLa_2(MoO_4)_4$: Er^{3+} have not being detected. The UC intensity of (d) $CaLa_2(MoO_4)_4$: Er^{3+}/Yb^{3+}# is much higher than that of (c) $CaLa_2(MoO_4)_4$: Er^{3+}/Yb^{3+} particles. Similar results are also observed from Er^{3+}/Yb^{3+} co-doped in other host matrices, which are assigned in the UC emission spectra with the green emission intensity ($^2H_{11/2} \rightarrow {}^4I_{15/2}$ and $^4S_{3/2} \rightarrow {}^4I_{15/2}$ transitions) and the red emission intensity ($^4F_{9/2} \rightarrow {}^4I_{15/2}$ transition) [7, 10, 26-28]. The doping amounts of Er^{3+}/Yb^{3+} had a great effect on the morphological features of the particles and their UC fluorescence intensity. The Yb^{3+} ion sensitizer can be effectively

excited by the energy of the incident light source, which transfers this energy to the activator, where radiation can be emitted. The Er^{3+} ion activator is the luminescence center in UC particles, and the sensitizer enhances the UC luminescence efficiency.

Fig. 5 shows the Raman spectra of the synthesized (a) $CaLa_2(MoO_4)_4$ (CLM), (b) $CaLa_2(MoO_4)_4$: Er^{3+} (CLM:Er), (c) $CaLa_2(MoO_4)_4$: Er^{3+}/Yb^{3+} (CLM:ErYb), and (d) $CaLa_2(MoO_4)_4$: Er^{3+}/Yb^{3+}# (CLM:ErYb#) particles excited by the 514.5-nm line of an Ar ion laser at 0.5 mW on the samples. The internal modes for the (a) $CaLa_2(MoO_4)_4$ (CLM) particles were detected at 318, 357, 380, 766, 838 and 906 cm^{-1}, respectively. The well-resolved sharp peaks for the $CaLa_2(MoO_4)_4$ particles indicate the high crystallinity state of the synthesized particles. The internal vibration mode frequencies are dependent on the lattice parameters and the degree of the partially covalent bond between the cation and molecular ionic group $[MoO_4]^{2-}$. The Raman spectra of the (b) $CaLa_2(MoO_4)_4$: Er^{3+} (CLM:Er), (c) $CaLa_2(MoO_4)_4$: Er^{3+}/Yb^{3+} (CLM:ErYb), and (d) $CaLa_2(MoO_4)_4$:Er^{3+}/Yb^{3+}# (CLM:ErYb#) particles indicate the domination of strong peaks at higher frequencies (1026, 1092 and 1316 cm^{-1}) and weak peaks at lower frequencies (236, 288, 365, 420 and 560 cm^{-1}). The Raman spectra of $CaLa_2(MoO_4)_4$: Er^{3+}, $CaLa_2(MoO_4)_4$:Er^{3+}/Yb^{3+} and $CaLa_2(MoO_4)_4$: Er^{3+}/Yb^{3+}# particles proved that the doping ions can influence the structure of the host materials. The combination of a heavy metal cation and the large inter-ionic distance for Er^{3+} and Yb^{3+} substitutions in La^{3+} sites in the lattice result in low probability of UC and the phonon-splitting relaxation in $CaLa_2(MoO_4)_4$ crystals. It could be considered that the very strong and strange effect may be generated by the disorder of the $[MoO_4]^{2-}$ groups with the incorporation of the Er^{3+} and Yb^{3+} elements into the crystal lattice or by a new phase formation.

Conclusions

The $CaLa_2(MoO_4)_4$: Er^{3+}/Yb^{3+} UC phosphors were successfully synthesized via cyclic microwave-modified sol-gel route. Well-crystallized $CaLa_2(MoO_4)_4$: Er^{3+}/Yb^{3+}# particles formed after heat-treatment at 900°C for 12 h showed a fine and homogeneous morphology with particle sizes of 1-3 μm. With excitation at 980 nm, $CaLa_2(MoO_4)_4$: Er^{3+}/Yb^{3+}# particles exhibited a strong 525-nm emission band and a weak 550-nm emission band in the green region, which were assigned to the $^2H_{11/2} \rightarrow {}^4I_{15/2}$ and $^4S_{3/2} \rightarrow {}^4I_{15/2}$ transitions, respectively, while a very weak 655-nm emission band in the red region was assigned to the $^4F_{9/2} \rightarrow {}^4I_{15/2}$ transition. The UC intensity of $CaLa_2(MoO_4)_4$: Er^{3+}/Yb^{3+}# particles was much higher than those of the $CaLa_2(MoO_4)_4$: Er^{3+} and $CaLa_2(MoO_4)_4$:Er^{3+}/Yb^{3+} particles. The Raman spectra of $CaLa_2(MoO_4)_4$:Er^{3+}, $CaLa_2(MoO_4)_4$:Er^{3+}/Yb^{3+} and $CaLa_2(MoO_4)_4$:Er^{3+}/Yb^{3+}# particles indicated the domination of strong peaks at higher frequencies (1026, 1092 and 1316 cm^{-1}) and weak peaks at lower frequencies (236, 288, 365, 420 and 560 cm^{-1}) induced by the disorder of the $[MoO_4]^{2-}$ groups with the incorporation of the Er^{3+} and Yb^{3+} elements into the crystal lattice or by a new phase formation.

Acknowledgement

This study was supported by Basic Science Research Program through the National Research Foundation of Korea (NRF) funded by the Ministry of Education, Science and Technology (2013-054508).

References

[1] M. Wang, G. Abbineni, A. Clevenger, C. Mao, S. Xu, *Nanomedicine: Nanotech. Biology, and Medicine*, **7**, 710 (2011).

[2] A. Shalav, B.S. Richards, M.A. Green, *Solar Ener. Mat. Solar Cells*, **91,** 829 (2007).

[3] C. Zhang, L. Sun, Y. Zhang, C. Yan, *J. Rare Earths*, **28**, 807 (2010).

[4] J. Liao, D. Zhou, B. Yang, R. liu, Q. Zhang, Q. Zhou, *J. Lum*., **134**, 533 (2013).

[5] J. Sun, Y. Lan, Z. Xia, H. Du, *Opt. Mat*., **33**, 576 (2011).

[6] C. Guo, H. K. Yang, J.H. Jeong, *J. Lum*., **130**, 1390 (2010).

[7] J. Sun, J. Xian, H. Du, *J. Phys. Chem. Solids*, **72**, 207 (2011).

[8] V.K. Komarala, Y. Wang, M. Xiao, *Chem. Phys. Lett*., **490**, 189 (2010).

[9] J. Sun, J. Xian, Z. Xia, H. Du, *J. Rare Earths*, **28**, 219 (2010).

[10] H. Du, Y. Lan, Z. Xia, J. Sun, *Mat. Res. Bull*., **44**, 1660 (2009).

[11] L.X. Pang, H. Liu, D. Zhou, G.B. Sun, W.B. Qin, W.G. Liu, *Mat. Lett*., **72**, 128 (2012).

[12] M. Haque, D.K. Kim, *Mat. Lett*., **63**, 793 (2009).

[13] V.V. Atuchin, O.D. Chimitova, S.V. Adichtchev, J.G. Gazarov, T.A. Gavrilova, M.S. Molokeev, N.S. Surovtsev, Zh.G. Bazarova, *Mat. Lett*., **106**, 26 (2013).

[14] L. Qin, Y. Huang, T, Tsuboi, H.J. Seo, *Mat. Res. Bull*., **47**, 4498 (2012).

[15] Y.L. Yang, X.M. Li, W.L. Feng, W.L. Li, C.Y. Tao, *J. Alloy Comps*., **505**, 239 (2010) .

[16] Y. Tian, B. Chen, B. Tian, R. Hua, J. Sun, L. Cheng, H. Zhong, X. Li, J. Zhang, Y. Zheng, T. Yu, L. Huang, Q. Meng, *J. Alloy Comps*., **509**, 6096 (2011).

[17] Y. Huang, L. Zhou, Z. Tang, *Opt. Mat*., **33**, 777 (2011).

[18] Y. Tian, B. Chen, B. Tian, J. Sun, X. Li, J. Zhang, L. Cheng, H. Zhong, H. Zhong, Q. Meng, R. Hua, *Physica B*, **407**, 2556 (2012).

[19] J. Liao, H. You, D. Zhou, H.R. Wen, R. Hong, *Opt. Mat*., **34**, 1468 (2012).

[20] Q. Chen, L. Qin, Z. Feng, R. Ge, X. Zhao, H. Xu, *J. Rare Earths*, **29**, 843 (2011).

[21] X. Shen, L. Li, F. He, X. Meng, F. Sing, *Mat. Chem. Phys*., **132**, 471 (2012).

[22] J. Zhang, X. Wang, X, Zhang, X. Zhao, X. Liu, L. *Peng, Inog. Chem. Comm.,* **14**, 1723 (2011).

[23] S. Das, A.K. Mukhopadhyay, S. Datta, D. Basu, *Bull. Mat. Sci*., **3**, 1 (2009).

[24] T. Thongtem, A. Phuruangrat, S. Thongtem, *J. Nanopart. Res*., **12**, 22287 (2010).

[25] V. Thangadurai, C. Knittlmayer, W. Weppner, *Mat. Sci. Eng. B*, **106**, 228 (2004).

[26] C. S. Lim, *Mat. Res. Bull.* **47**, 4220 (2012).

[27] W. Lu, L. Cheng, J. Sun, H. Zhong, X. Li, Y. Tian, J. Wan, Y. Zheng, L. Huang, T. Yu, H. Yu, B. *Chen, Physica B*, **405**, 3284 (2010).

[28] J. Sun, B. Sue, H. Du, *Infrar. Phys. Tech*., **60**, 10 (2013).